

Integrated microwave photonic devices based on graphene for the next generation wireless links

Alberto Montanaro
PNT Lab - CNIT

Via G. Moruzzi,1 56124 - Pisa, Italy
amontanaro@cnit.it

Matteo Tiberi

Cambridge Graphene Centre

9 JJ Thomson Ave, Cambridge, UK
mt840@cam.ac.uk

Alex Boschi

Center for Nanotechnology Innovation

@NEST, IIT
Piazza San Silvestro 12, 56127 Pisa, Italy
alex.boschi@iit.it

Guillaume Ducournau

CNRS, Univ. Polytech. Hauts de France
UMR 8520

Lille, France
guillaume.ducournau@univ-lille.fr

Vaidotas Mišeikis

Center for Nanotechnology Innovation
@NEST, IIT

P.zza S. Silvestro 12, 56127 Pisa, Italy
vaidotas.miseikis@iit.it

Stefano Soresi

Inphotec, CamGraPhIC srl

Via G. Moruzzi,1 56124 - Pisa, Italy
stefano.soresi@camgraphic-technology.com

Sara Pascale

Inphotec, CamGraPhIC srl

Via G. Moruzzi,1 56124 - Pisa, Italy
sara.pascale@camgraphic-technology.com

Chao Wen

Cambridge Graphene Centre

9 JJ Thomson Ave, Cambridge, UK
cw777@cam.ac.uk

Jincan Zhang

Cambridge Graphene Centre

9 JJ Thomson Ave, Cambridge, UK
jz543@cam.ac.uk

Mario Giovanni Frecassetti

NOKIA X-Haul BU

via Energy Park 14, 20871 Vimercate, Italy
mario_giovanni.frecassetti@nokia.com

Paola Galli

NOKIA Solutions and Networks Italia

City, Country
paola.galli@nokia.com

Henri Happy

IEMN, Université de Lille

Lille, France
henri.happy@univ-lille.fr

Sergio Pezzini

NEST, Istituto Nanoscienze-CNR
and Scuola Normale Superiore

P.zza S. Silvestro 12, 56127 Pisa, Italy
sergio.pezzini@nano.cnr.it

Andrea C. Ferrari

Cambridge Graphene Centre

9 JJ Thomson Ave, Cambridge, UK
acf26@cam.ac.uk

Marco Romagnoli

Inphotec, CamGraPhIC srl

Via G. Moruzzi,1 56124 - Pisa, Italy
marco.romagnoli@camgraphic-technology.com

Camilla Coletti

Center for Nanotechnology Innovation
@NEST, IIT

Piazza San Silvestro 12, 56127 Pisa, Italy
camilla.coletti@iit.it

Vito Sorianello

PNT Lab - CNIT

Via G. Moruzzi,1 56124 - Pisa, Italy
vito.sorianello@cnit.it

Abstract—We present sub-THz links using graphene-based integrated photodetectors in the photobolometric regime. We use these as optoelectronic mixers to reduce the complexity of common photonic-aided schemes, by eliminating the need of optical modulators, commonly used to encode the data stream in the optical domain. We use them as photonic-aided sub-THz up-converters and down-converters, with bandwidth covering the entire W-band range.

Index Terms—graphene, integrated photonics, high speed detectors, optoelectronic mixing, sub-THz links

I. INTRODUCTION

The next generation communication standards such as the 6G technology will require multi-Gbit/s data-rate links [1]

to afford the demand of high-bandwidth (BW) in the GHz range, low-latency ($\sim \mu\text{s}$ range) networks with maximized number of connected devices [1]. To increase the electrical BW of the wireless channels, mm-wave and sub-THz carriers will be used [1]. The generation, processing and detection of such frequencies can be achieved using microwave photonics, allowing BW operation and wide tuneability in the mm-wave and sub-THz range and extremely stable radio-frequency (RF) generation [2] with phase noise $\ll 100$ dBc/Hz at frequencies < 1 MHz from the sub-THz carrier frequency [3]. Up- and down-conversion are crucial at both the transmitter and receiver stage [4]. To achieve this, different schemes have been proposed, mainly relying on modulators cascaded with ultra-

fast photodiodes [5]. Most are bulky [6], thus not suitable to realize antenna arrays. Owing to broadband optical absorption [7], short photocarriers lifetime [8], and compatibility with the standard silicon technological [9], graphene can be used as the active material to realize ultra-fast photonic-aided up- and down-converters [10] that can operate at several hundreds of GHz. These devices are particularly interesting if small footprints (lower than the carrier frequency wavelength) are required, such as for antenna arrays. Here, we present integrated optoelectronic mixers based on graphene as W-band up-converters and down-converters.

II. PHOTONIC-AIDED SUB-THZ WIRELESS LINKS

A typical photonic based sub-THz wireless link is implemented using a laser source with frequency f_1 modulated with some base-band information using an optical modulator [4]. The modulated signal is coupled to a photodiode (with BW > 100 GHz for W-band operation) together with a second laser with frequency $f_2 = f_1 + \Delta f$. Δf lies in the sub-THz range [4]. The beating of the two lasers produces a signal at Δf , then transmitted through the wireless link. A photonic-aided receiver can be used as well. This can be implemented with, e.g., ultra-broadband (BW > 100 GHz for W-band operation) modulators [11]. These schemes involve, at both receiver and transmitter, a double conversion of the data stream, encoded from the electrical to the optical domain, and then back again to the electrical domain. Each conversion involves losses, and moreover the use of two optoelectronic components (modulator and detector) makes very difficult the integration of this architecture in a small area [6] comparable with the carrier frequency wavelength. Thus, for systems requiring reduced footprints (like, e.g. antenna arrays), the electronic solution is by far the most preferred one [12]. Graphene photodetectors (PDs) can overcome this limitation, since they do not require optical modulators by providing self-mixing functionalities [10], with footprints smaller than the typical size ($< \text{mm}^2$ range) of a single antenna element of a sub-THz system [10]. The working principle of graphene optoelectronic mixers relies is the change in conductivity of single layer graphene (SLG) induced by light absorption [6], [13]:

$$\sigma_{light} = \sigma_{dark} + \Delta\sigma \quad (1)$$

Which results in a change in the channel resistance:

$$R_{light} = \left(\frac{1}{R_{dark}} + \frac{1}{\Delta R} \right)^{-1} \quad (2)$$

Where $R_{dark} = \frac{L}{W} \frac{1}{\sigma_{dark}}$, $\Delta R = \frac{L}{W} \frac{1}{\Delta\sigma}$, being W the width and L the length of the SLG channel [6], [13]. A time-varying change in conductivity is produced if two lasers with frequency f_1 and f_2 beat on a SLG PD, so the resulting resistance is:

$$\Delta R = \frac{L}{W} \frac{1}{\Delta\sigma} = \frac{L}{W} \frac{1}{\delta\sigma + \delta\sigma \sin(2\pi\Delta f t)} \quad (3)$$

with $\Delta f = |f_1 - f_2|$.

Since the SLG photocarriers relaxation dynamics is in the ps range [14], this conductivity change can reach several hundred GHz [9]. The application of an electrical signal $V_{in} = \widetilde{V}_{in} \sin(2\pi f_{ele} t)$ over the time-varying resistance produces a modulation term [6]:

$$\begin{aligned} & \widetilde{V}_{in} \sin(2\pi f_{ele} t) \delta\sigma \sin(2\pi\Delta f t) = \\ & \frac{\widetilde{V}_{in} \delta\sigma}{2} [\cos(2\pi|\Delta f - f_{ele}|t) + \cos(2\pi(\Delta f + f_{ele})t)] \end{aligned} \quad (4)$$

Therefore the device can be used as both up- and down-converter in the sub-THz range.

III. RESULTS AND DISCUSSION

Fig.1a shows a representative device, while a cross-section is shown in Fig.1b. SLG or Bi-layer graphene (BLG) grown by chemical vapour deposition (CVD) is transferred on a silicon nitride (SiN) photonic waveguide (WG), embedded into an electrical RF coplanar waveguide (CPW). The graphene region is encapsulated using different dielectrics, such as Al_2O_3 [15] or hexagonal boron nitride (hBN) [16]. A second SLG is used as electrostatic gate to set optimal operation [6]. With reference to Fig.1c, the CPW is used to feed the electrical signal from one side, and to recover the up- or down-converted signal from the other side using RF probes. Due to the symmetry of the device, both sides can be used as RF or IF ports. The frequency conversion process is triggered by the application of an optical local oscillator (LO port) consisting in two wavelengths separated by Δf lying in the W-band. The design (comprising WG geometry, channel length and width, distance between WG and SLG or BLG and RF CPW geometry) follows the design rules of Ref. [6]. A multi-physics simulation is used to calculate optical mode and hot-electrons temperature profile along the channel upon optical coupling, directly linked to the photo response of SLG or BLG photobolometers [17]. These simulations provide the optimal SLG or BLG channel geometry considering the amount of optical absorption, channel resistance and optical losses due to metal contacts. The laser source is coupled to the devices through vertical coupling with standard single mode fibers and a grating coupler, or via a lensed fiber, butt coupled through an inverse taper edge coupler.

Fig.2a shows the characterization of the frequency response of a representative SLG PD, performed by applying a constant DC voltage across the device structure, and measuring the photocurrent generated by coupling a dual wavelength laser source to the device. This is realized using a 40GHz phase modulator generating a frequency comb starting from a constant wavelength (CW) laser source. Two lines out of the comb are selected using an optical wave shaper. The frequency separation of the two optical lines is swept between 65 and 110GHz. The resulting frequency response is measured using a W-band power meter. The flat response shows that the device can be operated over the entire W-band. The setup losses, comprising RF probes operating in the W-band, RF cables and transitions, and one RF amplifier, are characterized prior to the measurements.

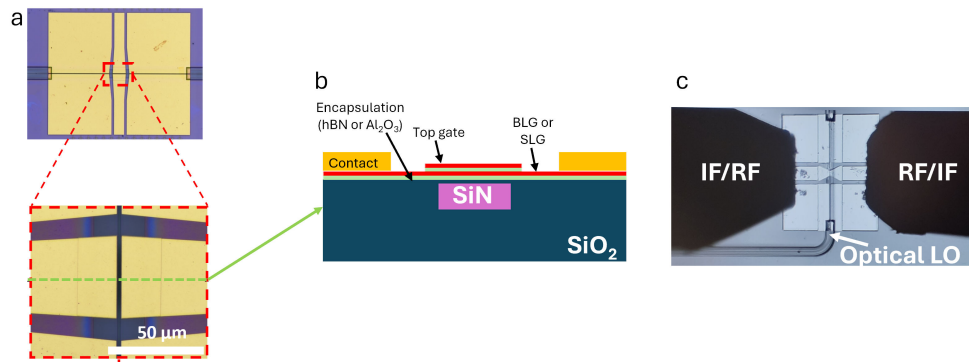


Fig. 1. Top (a) and transverse (b) GOEM layout. c) : GOEM ports

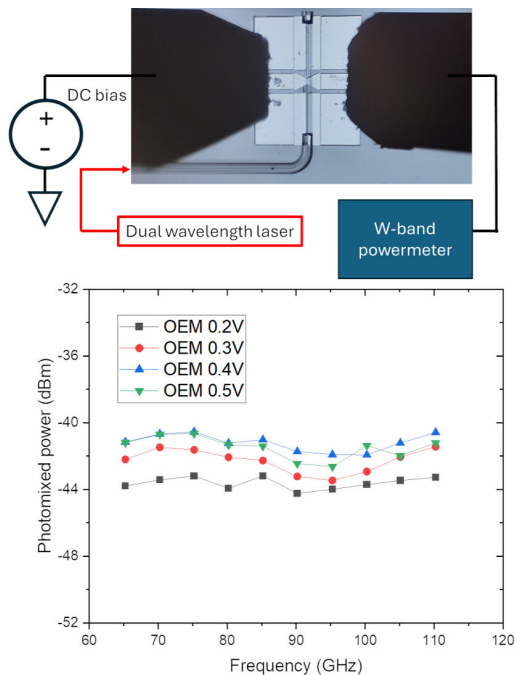


Fig. 2. Device frequency response in the W-band

We then test the devices in the W-Band range as up-converters, Fig.3, with datastreams applied to the devices, and upconverted using the same dual wavelength laser source described above, set at two different frequencies, i.e. 80 and 90GHz. The upconverted signal is coupled to a commercial W-band receiver connected to a real time oscilloscope. A difference in the error vector magnitude (EVM) between the 90GHz carrier frequency (CF) datastream and the 80GHz CF datastream is observed, attributed to the W-band receiver limited BW.

A characterization of the devices used as down-converters is reported in Fig.4. W-band electrical signals in the range 80-99.9GHz are generated by photomixing two lasers on a commercial photodiode with $BW \sim 110GHz$ and coupled to the RF port of the SLG-OEM. Then, the dual wavelength laser source is set to 100GHz, and the resulting down-converted

signal in the range [0.1-20GHz] is measured. The response is flat over the whole range, enabling this device to be used as receiver in a W-band wireless link.

IV. CONCLUSIONS

We presented a photonic-aided frequency converter that can be used in W-band wireless links at both the transmitter and receiver stage with multi Gbit/s operation. Compared to the classic photonic implementations, our approach allows for drastic footprint reduction down to $< 1mm^2$. Compared to the electronic implementations, it has the advantages of optically-based RF signal generation, like low phase noise ($\ll 100$ dBc/Hz at frequencies < 1 MHz from the sub-THz carrier frequency), electromagnetic immunity, and agile frequency tuneability. This makes our devices particularly suitable for next-generation antenna array systems.

ACKNOWLEDGMENT

We acknowledge funding from EU Horizon Europe research and innovation programme, through GraPh-X under grant 101070482, ERC Grants Hetero2D, GSYNCOR, GIP, EP-SRC Grants EP/K01711X/1, EP/K017144/1, EP/N010345/1, EP/L016087/1. We acknowledge Prof. K. Watanabe and Prof. T. Taniguchi for having provided the hBN crystals for the fabrication of BLG devices. The authors acknowledge Prof. Emiliano Pallecchi for the fruitful discussion on nonlinear graphene conductivity modelling.

REFERENCES

- [1] Tripathi, S. 6G Mobile Wireless Networks. (Springer International Publishing,2021)
- [2] Ghelfi, P., Laghezza, F., Scotti, F., Serafino, G., Capria, A., Pinna, S., Onori, D., Porzi, C., Scaffardi, M., Malacarne, A., Vercesi, V., Lazeri, E., Berizzi, F. & Bogoni, A. A fully photonics-based coherent radar system. *Nature*. **507**, 341 (2014,3), <http://dx.doi.org/10.1038/nature13078>
- [3] Tetsumoto, T., Nagatsuma, T., Fermann, M., Navickaite, G., Geiselmann, M. & Rolland, A. Optically referenced 300 GHz millimetre-wave oscillator. *Nature Photonics*. **15**, 516-522 (2021,7,1), <https://doi.org/10.1038/s41566-021-00790-2>
- [4] Koenig, S., Lopez-Diaz, D., Antes, J., Boes, F., Henneberger, R., Leuther, A., Tessmann, A., Schmogrow, R., Hillerkuss, D., Palmer, R., Zwick, T., Koos, C., Freude, W., Ambacher, O., Leuthold, J. & Kallfass, I. Wireless sub-THz communication system with high data rate. *Nature Photonics*. **7**, 977-981 (2013,12)

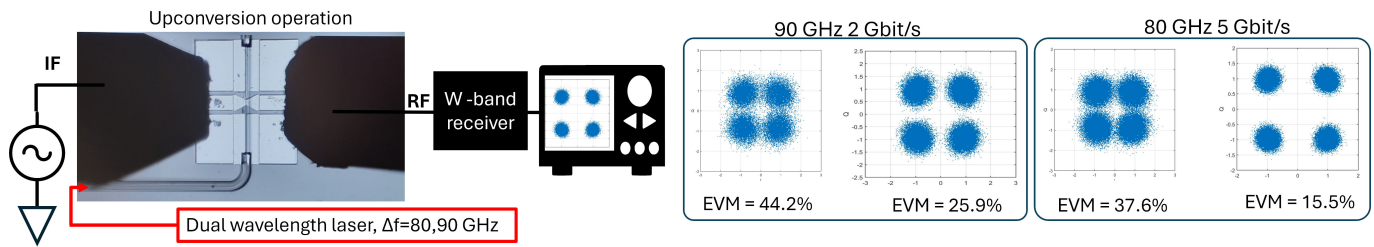


Fig. 3. Setup for up-conversion of data-streams and experimental results on a representative BLG-OEM

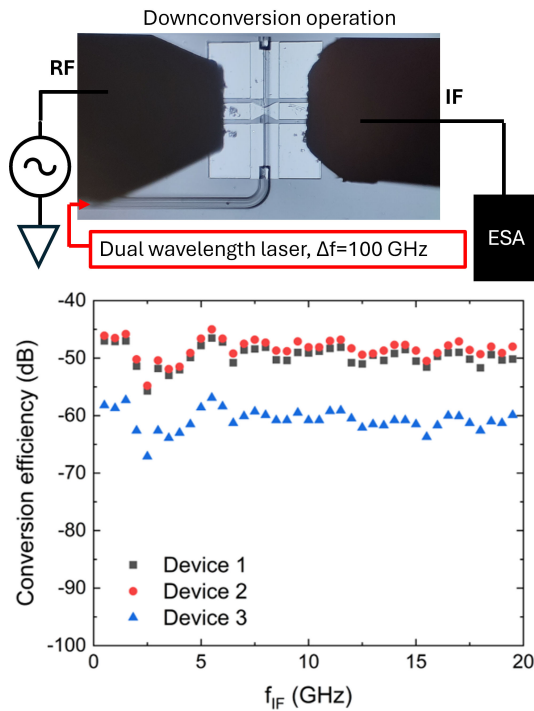


Fig. 4. GOEM characterization as W-band frequency down-converter

[5] Yu, X., Jia, S., Hu, H., Galili, M., Morioka, T., Jepsen, P. & Oxenløwe, L. 160 Gbit/s photonics wireless transmission in the 300-500 GHz band. *APL Photonics*. **1**, 081301 (2016,11)

[6] Montanaro, A., Piccinini, G., Mišeikis, V., Sorianello, V., Giambra, M., Soresi, S., Giorgi, L., D'Errico, A., Watanabe, K., Taniguchi, T. & Others Sub-THz wireless transmission based on graphene-integrated optoelectronic mixer. *Nature Communications*. **14**, 6471 (2023)

[7] Nair, R., Blake, P., Grigorenko, A., Novoselov, K., Booth, T., Stauber, T., Peres, N. & A. K. Geim Fine Structure Constant Defines Visual Transparency of Graphene. *Science*. **320**, 1308-1308 (2008), <https://www.science.org/doi/abs/10.1126/science.1156965>

[8] Brida, D., Tomadin, A., Manzoni, C., Kim, Y., Lombardo, A., Milana, S., Nair, R., Novoselov, K., Ferrari, A., Cerullo, G. & Polini, M. Ultrafast collinear scattering and carrier multiplication in graphene. *Nature Communications*. **4**, 1987 (2013,6), <https://doi.org/10.1038/ncomms2987>

[9] Romagnoli, M., Sorianello, V., Midrio, M., Koppens, F., Huyghebaert, C., Neumaier, D., Galli, P., Templ, W., D'Errico, A. & Ferrari, A. Graphene-based integrated photonics for next-generation datacom and telecom. *Nature Reviews Materials*. **3**, 392-414 (2018,10)

[10] Montanaro, A., Mzali, S., Mazellier, J., Bezencenet, O., Larat, C., Molin, S., Morvan, L., Legagneux, P., Dolfi, D., Dlubak, B., Senneor, P., Martin, M., Hofmann, S., Robertson, J., Centeno, A. & Zurutza, A. Thirty Gigahertz Optoelectronic Mixing in Chemical Vapor Deposited Graphene. *Nano Letters*. **16**, 2988-2993 (2016,5),

<http://dx.doi.org/10.1021/acs.nanolett.5b05141>

[11] Burla, M., Hoessbacher, C., Heni, W., Haffner, C., Fedoryshyn, Y., Werner, D., Watanabe, T., Massler, H., Elder, D., Dalton, L. & Leuthold, J. 500 GHz plasmonic Mach-Zehnder modulator enabling sub-THz microwave photonics. *APL Photonics*. **4**, 056106 (2019,5), <https://doi.org/10.1063/1.5086868>

[12] Hindle, P. Comprehensive survey of commercial mmWave phased array companies *Microwave Journal*. <https://www.microwavejournal.com/articles/33357-comprehensive-survey-of-commercial-mmwave-phased-array-companies> (2020)

[13] Montanaro, A., Wei, W., Fazio, D., Sassi, U., Soavi, G., Aversa, P., Ferrari, A., Happy, H., Legagneux, P. & Pallecchi, E. Optoelectronic mixing with high-frequency graphene transistors. *Nature Communications*. **12**, 1-10 (2021)

[14] Tomadin, A., Hornett, S., Wang, H., Alexeev, E., Candini, A., Coletti, C., Turchinovich, D., Kläui, M., Bonn, M., Koppens, F., Hendry, E., Polini, M. & Klaas-Jan Tielrooij The ultrafast dynamics and conductivity of photoexcited graphene at different Fermi energies. *Science Advances*. **4**, eaar5313 (2018), <https://www.science.org/doi/abs/10.1126/sciadv.aar5313>

[15] Canto, B., Otto, M., Powell, M., Babenko, V., O'Mahony, A., Knoop, H., Sundaram, R., Hofmann, S., Lemme, M. & Neumaier, D. Plasma-Enhanced Atomic Layer Deposition of Al₂O₃ on Graphene Using Monolayer hBN as Interfacial Layer. *Advanced Materials Technologies*. **6**, 2100489 (2021), <https://onlinelibrary.wiley.com/doi/abs/10.1002/admt.202100489>

[16] Dean, C., Young, A., Meric, I., Lee, C., Wang, L., Sorgenfrei, S., Watanabe, K., Taniguchi, T., Kim, P., Shepard, K. & Hone, J. Boron nitride substrates for high-quality graphene electronics. *Nature Nanotechnology*. **5**, 722-726 (2010,10), <https://doi.org/10.1038/nnano.2010.172>

[17] Hamidouche, L., Montanaro, A., Rosticher, M., Grimaldi, E., Poupet, B., Taniguchi, T., Watanabe, K., Plaças, B., Baudin, E. & Legagneux, P. Optoelectronic mixing in high-mobility graphene. *ACS Photonics*. **8**, 369-375 (2020)